1

The galactic ecosystem

The Milky Way is largely empty. Stars are separated by some 2 pc in the solar neighborhood ($\rho_\star = 6 \times 10^{-2}\,\mathrm{pc}^{-3}$). If we take our Solar System as a measure, with a heliosphere radius of $\simeq$235 AU, stars and their associated planetary systems fill about 3×10^{-10} of the available space. This book deals with what is in between these stars: the interstellar medium (ISM). The ISM is filled with a tenuous hydrogen and helium gas and a sprinkling of heavier atoms. These elements can be neutral, ionized, or in molecular form and in the gas phase or in the solid state. This gas and dust is visibly present in a variety of distinct objects: HII regions, reflection nebulae, dark clouds, and supernova remnants. In a more general sense, the gas is organized in phases – cold molecular clouds, cool HI clouds, warm intercloud gas, and hot coronal gas – of which those objects are highly visible manifestations. This gas and dust is heated by stellar photons, originating from many stars (the so-called average interstellar radiation field), cosmic rays (energetic [$\sim$GeV] protons), and X-rays (emitted by local, galactic, and extragalactic hot gas). This gas and dust cools through a variety of line and continuum processes and the spectrum will depend on the local physical conditions. Surveys in different wavelength regions therefore probe different components of the ISM. This first chapter presents an inventory of the ISM with an emphasis on prominent objects in the ISM and the global structure of the ISM.

The interstellar medium plays a central role in the evolution of the Galaxy. It is the repository of the ashes of previous generations of stars enriched by the nucleosynthetic products of the fiery cauldrons in the stellar interiors. These are injected either with a bang, in a supernova explosion, or with a whimper, in the much slower moving winds of low-mass stars on the asymptotic giant branch. In this way, the abundances of heavy elements in the ISM slowly increase. This is part of the cycle of life for the stars of the Galaxy, because the ISM itself is the birthplace of future generations of stars. It is this constant recycling and its

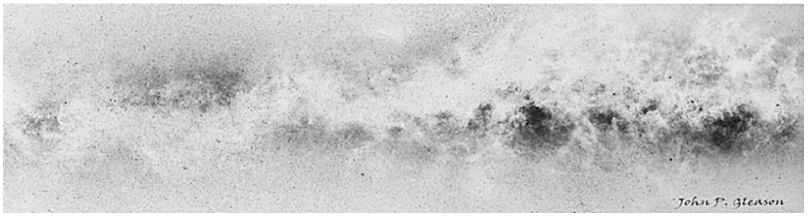

Figure 1.1 A panoramic image of a (southern) portion of the Milky Way's disk. The image has been inverted and dark corresponds to emission from ionized gas and reflection nebulae. The light band stretching irregularly across the whole image is due to absorption by dust clouds. Image courtesy of J. P. Gleason.

associated enrichment that drives the evolution of the Galaxy, both physically and in its emission characteristics.

1.1 Interstellar objects

1.1.1 HII regions

Ionized gas nebulae feature prominently in the Milky Way as bright visible nebulous objects. The Great Nebula in Orion (M42; Fig. 1.2) and the Lagoon Nebula (M8) are well-known examples. HII regions span a range in brightness, however, and fainter examples are the California Nebula and IC 434 (Fig. 1.3). The gas in these regions is ionized and has a temperature of about 10^4 K. Densities range from 10^3–10^4 cm^{-3} for compact ($\sim$0.5 pc) HII regions such as the Orion Nebula to $\sim$10 cm^{-3} for more diffuse and extended nebulae such as the North America Nebula ($\sim$10 pc). The optical spectra of these regions are dominated by H and He recombination lines and collisionally excited, optical (forbidden) line emission from trace ions such as [OII], [OIII], and [NII]. HII regions are also strong sources of thermal radio emission (free–free) from the ionized gas and of infrared emission due to warm dust. HII regions are formed by young massive stars with spectral type earlier than about B1 ($T_{\rm eff} > 25\,000$ K), which emit copious amounts of photons beyond the Lyman limit ($h\nu > 13.6$ eV) and ionize and heat their surrounding, nascent molecular clouds. They are, therefore, signposts of sites of massive star formation in the Galaxy.

1.1.2 Reflection nebulae

Reflection nebulae are bluish nebulae that reflect the light of a nearby bright star. NGC 2023 in the Orion constellation (see Fig. 1.3) and the striated nebulosity associated with the Pleiades are familiar cases. In this case, the observed light

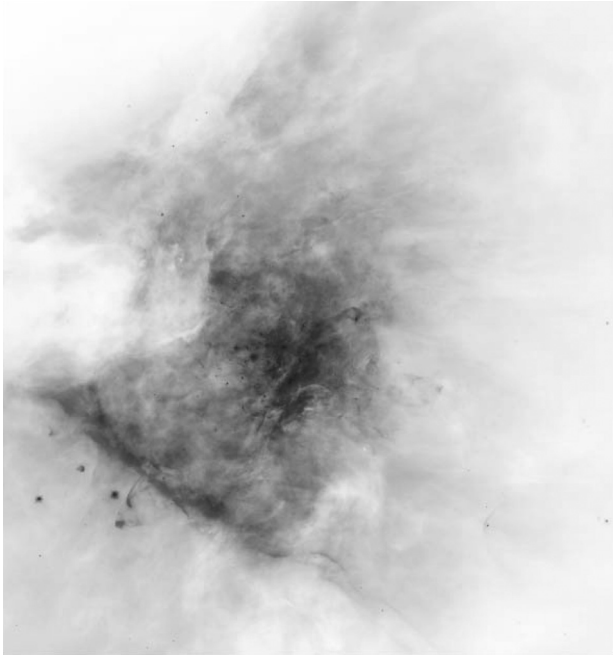

Figure 1.2 A black and white representation of the Orion Nebula as observed by the Hubble Space Telescope in [OIII], Hα, and [NII]. Light and dark have been inverted. The gas is ionized by the Trapezium cluster, in particular θ^1 C Ori, in the center of the image. The bright bar in the south-west is an ionization front eating its way into the surrounding neutral material in the photodissociation region known as the Orion Bar. The dark bay (light in this image), a cloud of foreground obscuring material, is also evident to the east. This image gives a clear view of the complex topography created by the interaction of a newly formed massive star with its surrounding natal cloud. Image courtesy of R. O'Dell.

is not due to hot gas but rather reflected starlight. There is no radio emission but there is infrared emission from warm dust, although this is less luminous than for HII regions. For the compact reflection nebulae, densities are typically a little smaller ($\simeq 10^3\,\mathrm{cm}^{-3}$) than for compact HII regions. Reflection nebulae are illuminated by stars with spectral types later than about B1. Regions around hotter stars also show (faint) reflected light emission but the spectrum is then dominated by the emission from the ionized gas. For the earlier stellar types, the surrounding nebulosity may be the material from which the star was formed (e.g., NGC 2023; NGC 7023). Often, however, the nebulosity is due to a chance encounter between the star and a cloud (e.g., the Pleiades). Reflection nebulae can also be associated with the ejecta of a late-type star (e.g., IC 2220; the Red Rectangle).

Figure 1.3 Part of the Orion molecular cloud containing the Horse Head Nebula. The diffuse glow behind the horse head is IC 434 ionized by the bright star, σ Ori. The horse head is a protrusion of the molecular cloud obvious in the lower part of this image. The nebula to the south-east of the horse head is the reflection nebula, NGC 2023. Image courtesy of the Canadian-France-Hawaii telescope, J.-C. Cuillandre, Coelem.

1.1.3 Dark nebulae

A striking aspect of the all-sky optical view of the Milky Way is the presence of many dark regions in which few stars are seen (cf. Fig. 1.1). The direction towards the center of the Galaxy is rampant with such dark clouds, which actually seem to divide the galactic plane in two. The Coalsack near the Southern Cross is a particularly nice example of a roundish dark cloud. Dark clouds are readily apparent when backlighted. The Horse Head Nebula (see Fig. 1.3) silhouetted against the reddish glow of the HII region, IC 434, and the dark bay in the Orion HII region (see Fig. 1.2) are two famous examples. Individual dark clouds come in a range of sizes from tens-of-parsecs large to the tiny ($\sim 10^{-2}$ pc) Bok globules associated with HII regions such as the Orion Nebula. Likewise, some dark clouds are completely black ($A_v > 10$ magnitudes) while others are hardly discernible. While dark clouds are outlined by the absence of stars, they do show faint optical

reflected light. Also, they become bright at mid- and far-infrared wavelengths. Some really dense clouds are opaque even at mid-IR wavelengths and appear as infrared dark clouds (IRDC) in absorption against background galactic mid-IR emission.

1.1.4 Photodissociation regions

While HII regions and reflection nebulae dominate the Galaxy at visible wavelengths, in the infrared, photodissociation regions dominate the sky. Originally, the name photodissociation regions (PDRs; sometimes also called photodominated regions with fortunately the same abbreviation) was given to the atomic–molecular zones that separate ionized and molecular gas near bright luminous O and B stars (e.g., surrounding HII regions and reflection nebulae) and the Orion Bar (Fig. 1.2) and NGC 2023 (Fig. 1.3) are prime examples of classical PDRs. In these regions, penetrating far-ultraviolet (FUV) photons (with energies between 6 and 13.6 eV) dissociate and ionize molecular species. Most of the FUV photons are absorbed by the dust, but a small fraction heat the gas through the photoelectric effect to a few hundred degrees. Photodissociation regions are thus bright in IR dust continuum and atomic fine-structure cooling lines as well as molecular lines. In essence, of course, everywhere where FUV photons strike a cloud, a PDR will ensue. Indeed, the term PDRs has now expanded to include all regions of the ISM where FUV photons dominate the physical and chemical processes. As such, PDRs include the neutral atomic gas of the ISM as well as much of the gas in molecular clouds (except, e.g., for dense starless cores).

1.1.5 Supernova remnants

Supernova remnants (SNRs) are formed when the material ejected in the explosion that terminates the life of some stars shocks surrounding ISM material and an SNR's spectrum is that of a high velocity shock. About 100 supernova remnants are visible in our Galaxy; they are generally characterized by long, delicate filaments radiating in-line radiation (Fig. 1.4). Supernova remnants are prominent sources of radio emission due to relativistic electrons spiraling around a magnetic field (synchroton emission) and some 200 have been identified at radio wavelengths. Supernova remnants also stick out at X-ray wavelengths because of emission by hot ($\simeq 10^6$ K) gas. Not all SNRs are wispy. The Crab Nebula is an example of a compact SNR.

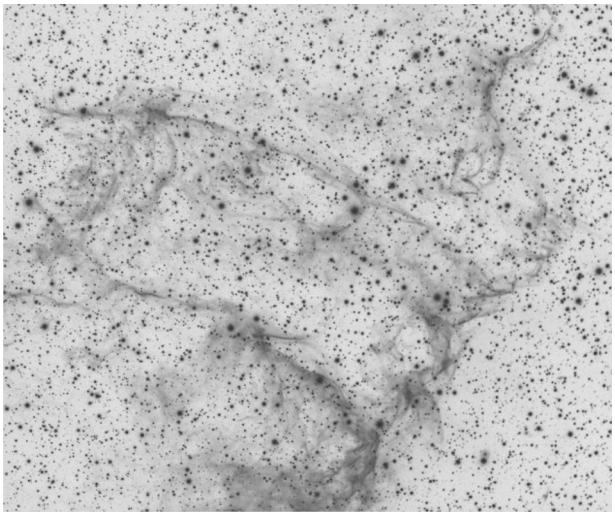

Figure 1.4 A small portion of the Cygnus Loop, the remnant of a supernova that exploded about 10 000 years ago. The image has been inverted to bring out the delicate structure of the nebulosity. The emission is due to a shock wave and is about 3 pc in size. Image courtesy of L. K. Tan, StarryScapes.

1.2 Components of the interstellar medium

The gas in the ISM is organized in a variety of phases. The physical properties of these phases are summarized in Table 1.1.

1.2.1 Neutral atomic gas

The 21 cm line of atomic hydrogen traces the neutral gas of the ISM. This neutral gas can also be observed in optical and UV absorption lines of various elements towards bright background stars. The neutral medium is organized in cold ($\simeq 100$ K) diffuse HI clouds (cold neutral medium, CNM) and warm (≈ 8000 K) intercloud gas (warm neutral medium, WNM). A standard HI cloud (often called a Spitzer-type cloud) has a typical density of 50 cm^{-3} and a size of 10 pc. The density of the WNM is much less ($\simeq 0.5\,\mathrm{cm}^{-3}$). Between 4 and 8 kpc from the galactic center, 80% of the HI mass in the plane of the Galaxy is in diffuse clouds in a layer with a (Gaussian) scale height of about 100 pc. At higher latitudes, however, much of the HI mass is in the intercloud medium with a larger scale height of 220 pc but with an exponential tail extending well into the lower halo. These two neutral phases have, on average, similar surface densities. Because the Sun is located in the local bubble, the local, total WNM column density towards the North Galactic Pole is about 2.5 times that of the CNM. In the outer Galaxy, the HI scale height rapidly increases.

Table 1.1 *Characteristics of the phases of the interstellar medium*

Phase	n_0^a (cm^{-3})	T^b (K)	ϕ_v^c (%)	M^d (10^9 $M_\odot$)	$< n_0 >^e$ (cm^{-3})	H^f (pc)	Σ^g ($M_\odot$pc^{-2})
Hot intercloud	0.003	10^6	∼50.0	—	0.0015	3000	0.3
Warm neutral medium	0.5	8000	30.0	2.8	0.1[h]	220[h]	1.5
					0.06[h]	400[h]	1.4
Warm ionized medium	0.1	8000	25.0	1.0	0.025[i]	900[i]	1.1
Cold neutral medium[j]	50.0	80	1.0	2.2	0.4	94	2.3
Molecular clouds	>200.0	10	0.05	1.3	0.12	75	1.0
HII regions	1–10^5	10^4	—	0.05	0.015[k]	70[k]	0.05

[a] Typical gas density for each phase.
[b] Typical gas temperature for each phase.
[c] Volume filling factor (very uncertain and controversial!) of each phase.
[d] Total mass.
[e] Average mid-plane density.
[f] Gaussian scale height, $\sim \exp[-(z/H)^2/2]$, unless otherwise indicated.
[g] Surface density in the solar neighborhood.
[h] Best represented by a Gaussian and an exponential.
[i] WIM represented by an exponential.
[j] Diffuse clouds.
[k] HII regions represented by an exponential.

1.2.2 Ionized gas

Diffuse ionized gas in the ISM can be traced through dispersion of pulsar signals, through optical and UV ionic absorption lines against background sources, and through emission in the Hα recombination line (see Fig. 1.5). The first two can only be done in a limited number of selected sight-lines. The faintness and large extent of the galactic Hα hamper the last probe. While most of the Hα luminosity of the Milky Way is emitted by distinct HII regions, almost all of the mass of ionized gas (10^9 $M_\odot$) resides in a diffuse component. This warm ionized medium (WIM) has a low density ($\simeq$0.1 cm^{-3}), a temperature of $\approx$8000 K, a volume filling factor of $\simeq$0.25, and a scale height of $\simeq$1 kpc. The weakness of the [OI] λ6300 line (in a few selected directions) implies that the gas is nearly fully ionized. The source of ionization is not entirely clear. Energetically, ionizing photons from O stars are the most likely candidates but these photons have to "escape" from the associated HII regions and travel over large distances (hundreds of parsecs)

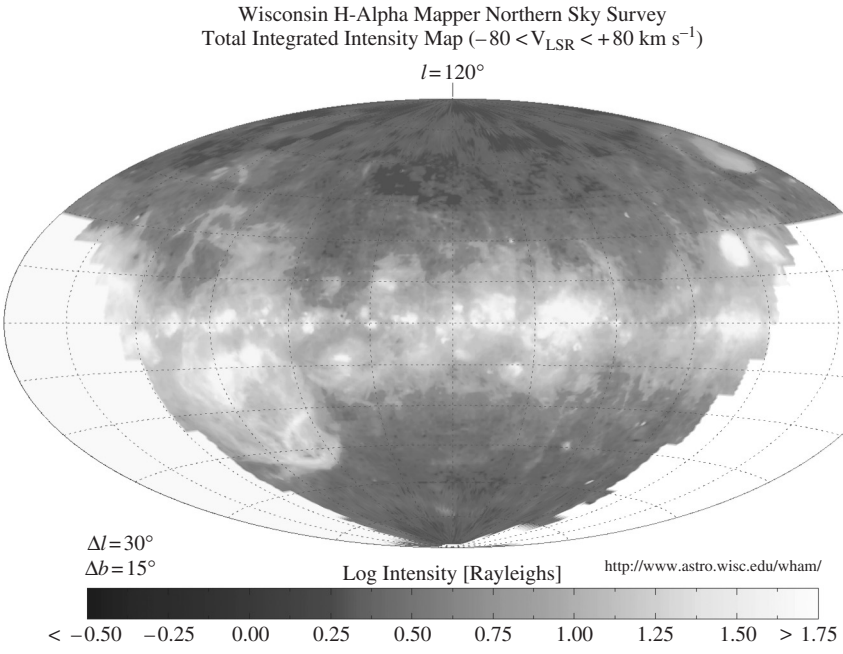

Figure 1.5 The integrated galactic (ℓ versus b) Hα emission obtained by the WHAM survey. This emission from ionized gas, about a million times fainter than the Orion Nebula, traces the warm ionized medium. Note the large filament (40°) sticking up out of the galactic plane. Image courtesy of R. Reynolds.

without being absorbed by omnipresent neutral hydrogen. Finally, the WIM shows a complex spatial structure including thin filaments sticking ~ 1 kpc out of the plane of the Galaxy, further compounding the ionization problem.

1.2.3 Molecular gas

The CO J = 1 − 0 transition at 2.6 mm is commonly used as a tracer of molecular gas in the Galaxy (Fig. 1.6). Surveys in this line have shown that much of the molecular gas in the Milky Way is localized in discrete giant molecular clouds with typical sizes of 40 pc, masses of 4×10^5 $M_\odot$, densities of $\simeq 200\,\mathrm{cm}^{-3}$, and temperatures of 10 K. However, it should be understood that molecular clouds show a large range in each of these properties. Molecular clouds are characterized by high turbulent pressures as indicated by the large linewidths of emission lines. Molecular clouds are self-gravitating rather than in pressure equilibrium with other phases in the ISM. While they are stable over time scales of $\simeq 3 \times 10^7$ years, presumably because of a balance of magnetic and turbulent pressure and gravity, molecular clouds are the sites of active star formation. Observations of molecular

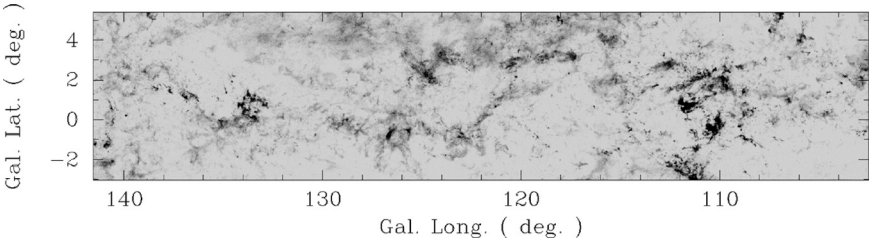

Figure 1.6 The emission of CO in the outer Galaxy obtained by the FCRAO survey. Much of the emission is local, stemming from molecular clouds between 0.5 and 1 kpc. In addition, giant molecular clouds associated with the NGC 7538-Sharpless 156-Sharpless 152 region ($\ell = 110°$) and the W3-W4-W5 region ($\ell = 135°$) are also present. The image has been inverted and dark corresponds to emission. Image courtesy of Chris Brunt (FCRAO).

clouds in the rotational transitions of a variety of species allow a detailed study of their physical and chemical properties. These studies show that molecular clouds have spatial structure on all scales. In particular, molecular clouds contain cores with sizes of $\simeq 1$ pc, densities in excess of 10^4 cm^{-3}, and masses in the range 10–10^3 $M_\odot$ in which star formation is localized. While CO is commonly used to trace interstellar molecular gas, H_2 is thought to be the dominant molecular species, with a H_2/CO ratio of 10^4–10^5. In addition, some 200 different molecular species have been detected – mainly through their rotational transitions in the submillimeter wavelength regions – in the shielded environments of molecular clouds. In general, these species are relatively simple, often unsaturated, radicals, or ions. Acetylenic carbon chains and their derivatives figure prominently on the list of detected molecules. However, this may merely reflect observational bias, since such species possess large dipole moments and relatively small partition functions, both of which make them readily detectable at microwave wavelengths.

1.2.4 Coronal gas

Hot ($\sim 10^5$–10^6 K) gas can be traced through UV absorption lines of highly ionized species (e.g., CIV, SVI, NV, OVI) seen against bright background sources. Such hot plasmas also emit continuum (bremsstrahlung, radiative recombination, two photon) and line (collisionally excited and recombination) radiation in the extreme ultraviolet and X-ray wavelength regions. These observations have revealed the existence of a pervasive hot ($3–10 \times 10^5$ K) and tenuous ($\simeq 10^{-3}$ cm^{-3}) phase (the hot intercloud medium, HIM) of the ISM. The observations indicate a range of temperatures where the higher ionization stages probe hotter gas. The hot gas fills most of the volume of the halo (scale height $\simeq 3$ kpc) but the volume filling factor

in the disk is more controversial. This gas is heated and ionized through shocks driven by stellar winds from early type stars and by supernova explosions. Much of the hot, high-latitude gas may have been vented by superbubbles created by the concerted efforts of whole OB associations into the halo in the form of a galactic fountain. This hot gas cools down, "condenses" into clouds, and rains down again on the disk. In the disk, the distribution of the hot gas is quite irregular. The Sun itself is located in a hot bubble with a size of approximately 100 pc.

1.2.5 Interstellar dust

The presence of dust in the interstellar medium manifests itself in various ways. Through their absorption and scattering, small dust grains give rise to a general reddening and extinction of the light from distant stars (Fig. 1.1). Moreover, polarization of starlight is caused by elongated large dust grains aligned in the galactic magnetic field (dichroic absorption). Furthermore, near bright stars, scattering of starlight by dust produces a reflection nebula. Finally, the interstellar medium is bright in the infrared because of continuum emission by cold dust grains. Analysis of the wavelength dependence of interstellar reddening implies a size distribution, $n(a) \sim a^{-3.5}$, which ranges from $\simeq$3000 Å all the way to the molecular domain ($\sim$5 Å). The number density of grains with sizes $\sim$1000 Å is $\simeq 10^{-13}$ per H atom. Most of the mass of interstellar dust is thus in the larger grains but the surface area is in the smallest grains. Abundance studies in the ISM show that many of the refractory elements (e.g., C, Si, Mg, Fe, Al, Ti, Ca) are locked up in dust; i.e., dust contains about 1% by mass of the gas.

Large ($\gtrsim$100 Å) interstellar dust grains are in radiative equilibrium with the interstellar radiation field at temperatures of $\simeq$15 K and the absorbed stellar photons are reradiated as infrared and submillimeter continuum emission. Near bright stars, the dust temperature is higher; typically some 75 K for a compact HII region. Emission by interstellar dust dominates these wavelength regions. Rotating interstellar dust grains also give rise to emission at radio wavelengths. Very small ($\lesssim$100 Å) dust grains undergo fluctuations in their temperature upon the absorption of a single UV photon and emit at mid-IR (25–60 μm) wavelengths.

1.2.6 Large interstellar molecules

Besides dust grains, the interstellar medium also contains a population of large molecules. These molecules are particularly "visible" at mid-IR wavelengths. The IR spectrum of most objects – HII regions, reflection nebulae, surfaces of dark clouds, diffuse interstellar clouds and cirrus clouds, galactic nuclei, the interstellar

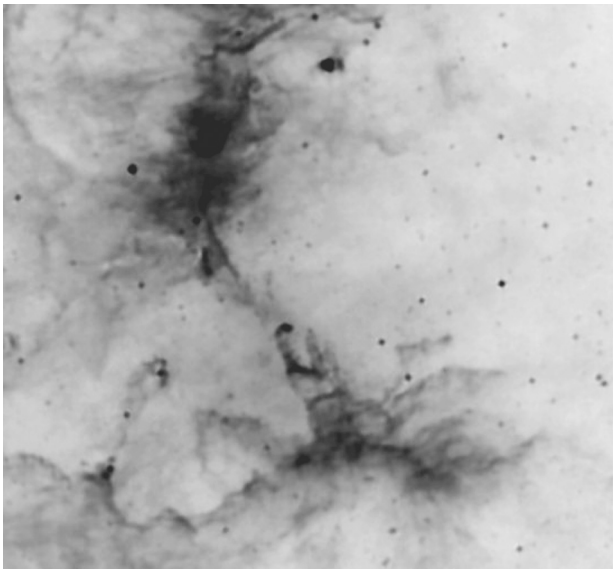

Figure 1.7 An infrared view of the Eagle Nebula (image inverted) obtained with ISOCAM on the Infrared Space Observatory. The dark emission that dominates the image is due to IR fluorescence of large polycyclic aromatic hydrocarbon molecules. Near the center of the image some of the faint emission is due to large, cool dust grains present in the ionized gas. The well-known pillars are visible just under the center of this image as the three-fingered hand. Image courtesy of the ISOGAL team, especially Andrea Moneti and Frederic Schuller.

medium of galaxies as a whole, and star burst galaxies – are dominated by broad infrared emission features (Fig. 1.7). These IR emission features are characteristics for polycyclic aromatic hydrocarbon (PAH) materials. These bands represent the vibrational relaxation process of FUV-pumped PAH species, containing some 50 C atoms. These species are very abundant, $\sim 10^{-7}$ relative to H, locking up about 10% of the elemental carbon.

These PAHs may just be one – very visible – representative of the molecular Universe. In fact, visible spectra of stars generally show prominent absorption features that are too broad to be atomic in origin. These so-called diffuse interstellar bands (DIBs) are generally attributed to electronic absorption by moderately large molecules (10–50 C atoms). Unsaturated carbon chains, containing 10–20 C atoms, are leading candidates for these DIBs. There are now in excess of 200 DIBs known, of which some 50 are moderately strong. Because, typically, the visible spectrum of a molecular species is dominated by at most one strong transition, the DIBs implicate the presence of a large number of different molecular species.

These large molecules seem to represent the extension of the interstellar grain size distribution into the molecular domain. Interstellar grains are known to contain

several populations of nano particles: nano diamonds have been isolated from meteorites with an isotopic composition that indicates a presolar origin; i.e., these grains predate the formation of the Solar System and they never fully equilibrated with the gas in the early solar nebula. Likewise, silicon nanoparticles may be the carrier of a widespread luminescence phenomena, the so-called extended red emission (ERE).

1.3 Energy sources

1.3.1 Radiation fields

The ISM is permeated by various photon fields, which influence the physical and chemical state of the gas and dust (Fig. 1.8). The stellar radiation field contains contributions from early-type stars, which dominate the far-ultraviolet (FUV)

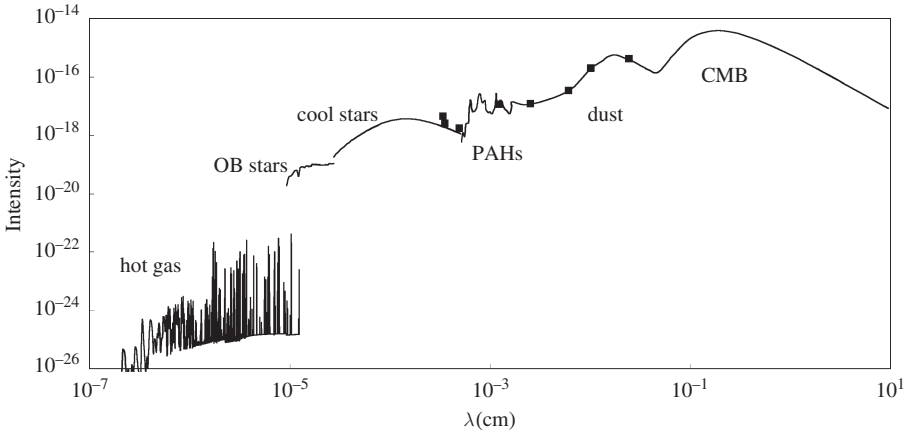

Figure 1.8 The mean intensity in units of erg cm^{-2} s^{-1} Hz^{-1} sr^{-1} of the interstellar radiation field in the solar neighborhood. Contributions by hot gas, OB stars, older stars, large molecules (PAHs), dust, and the cosmic microwave background are indicated. Figure adapted from J. Black, 1996, *First Symposium on the IR Cirrus and Diffuse Interstellar Clouds*, ed. R. M. Cutri and W. B. Latter (San Francisco: ASP), p. 355. The calculated X-ray/EUV emission spectrum and the FUV spectrum were kindly provided by J. Slavin. The dust emission is a fit to the COBE results for the galactic emission. The PAH spectrum was taken from ISO measurements of the mid-IR emission spectrum of the interstellar medium scaled to the measurements of the IR cirrus by IRAS (F. Boulanger, 2000, in *ISO Beyond Point Sources: Studies of Extended Infrared Emission*, ed. R. J. Laureijs, K. Leech, and M. F. Kessler, *E. S. A.-S. P.,* **455**, p. 3). The black squares at 12, 25, 60 and 100 μm are the IRAS measurements of the IR cirrus, the DIRBE/COM measurement at 240 μm, and those at 3.3, 3.5, and 4.95 μm are the balloon measurement by Proneas experiment (M. Giard, J. M. Lamarre, F. Pajot, and G. Serra, 1994, *A. & A.*, **286**, p. 203). Note that the latter have been superimposed on the stellar spectrum.

wavelengths, A-type stars, which control the visible region, and late-type stars, which are important at far-red to near-infrared wavelengths. The strength of the FUV average interstellar radiation is often expressed in terms of the Habing field, 1.2×10^{-4} erg cm^{-2} s^{-1} sr^{-1}, named after Harm Habing, a pioneer in this field. Current estimates put the average interstellar radiation field at $G_0 = 1.7$ Habing fields. Often, the radiation field in PDRs produced by a nearby star shining on a nearby cloud is expressed in terms of the equivalent one-dimensional average interstellar radiation field flux (e.g., 1.6×10^{-3} erg cm^{-2} s^{-1}).

These stellar photons are absorbed by dust grains and reradiated at longer wavelengths – in discrete emission bands in the mid-IR and in continuum emission in the far-IR and submillimeter regions (Fig. 1.8). The 2.7 K cosmological background takes over at millimeter wavelengths. At extreme ultraviolet wavelengths (EUV), even a small amount of neutral hydrogen absorbs all radiation and the intensity of the average radiation field due to stars drops precipitously at the Lyman edge (912 Å; Fig. 1.9). Stars do not contribute much at the shortest wavelengths (X-rays). Instead, emission by hot plasmas – the coronal gas in the halo and in SNRs – dominates the radiation field. This component shows numerous emission lines. There is also an extragalactic contribution at the hardest energies. These X-ray emission components are mediated by absorption by foreground

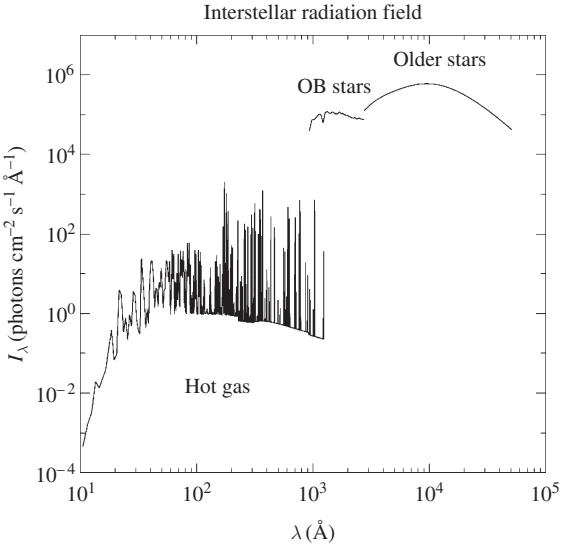

Figure 1.9 The average photon field in the solar neighborhood in units of photons cm^{-2} s^{-1} Å^{-1}. Contributions by hot gas, OB stars, and older stars are indicated. The calculated X-ray/EUV/FUV spectrum was kindly provided by J. Slavin. The visual spectrum was taken from J. S. Mathis, P. G. Mezger, and N. Panagia, 1983, *A. & A.*, **128**, p. 212.

Table 1.2 *Energy balance for diffuse clouds*

Source	P (10^{-12} dyne cm^{-2})	Energy density (eV cm^{-3})	Heating rate (erg s^{-1} H-atom^{-1})
Thermal	0.5	6.0	–5 (–26)[a]
UV	—	0.5	5 (–26)
Cosmic ray	1.0	2.0	3 (–27)
Magnetic fields	1.0	0.6	2 (–27)
Turbulence	0.8	1.5	1 (–27)
2.7 K background	—	0.25	—

[a] Energy loss rate.

gas and, because the ionization cross section decreases rapidly with increasing energy at EUV–X-ray wavelengths, this effect is more pronounced at the longer wavelengths.

Photodissociation rates and ionization rates are proportional to the photon intensity (Fig. 1.9). A simple polynomial fit for the mean photon intensity of the interstellar radiation field is

$$\mathcal{N}_{\rm ISRF} = 8.530\times10^{-5}\lambda^{-1} - 1.376\times10^{-1}\lambda^{-2} + 5.495\times10^{1}\lambda^{-3}\,{\rm cm^{-2}s^{-1}Hz^{-1}sr^{-1}}, \quad (1.1)$$

with λ in Å. The Habing field corresponds to about 10^8 photons cm^{-2} s^{-1} between 6 and 13.6 eV and about a factor of 10 fewer between 11 and 13.6 eV.

1.3.2 Magnetic fields

The magnetic field is an important energy and pressure source in the ISM (cf. Table 1.2), controlling to a large extent the dynamics of the gas. The interstellar magnetic field manifests itself through linear polarization of starlight by aligned dust grains (dichroic absorption; Fig. 1.10), in polarization of far-infrared continuum emission of aligned dust grains, linear polarization of synchroton emission, Faraday rotation of background, polarized, radio sources, and Zeeman splitting of the 21 cm HI line and lines of molecules with unpaired electrons such as OH.

The magnetic field is about 5 μG in the solar neighborhood, increasing to about 8 μG in the molecular ring at 4 kpc. Models for the synchroton emission, which trace the distribution of the magnetic field, imply the existence of a thin-disk component, associated with the gaseous disk, and a thick-disk component – the halo component – with a scale height of 1.5 kpc near the solar circle. The magnetic field consists of a uniform component and a non-uniform component. The uniform component of the magnetic field is roughly circular with a strength

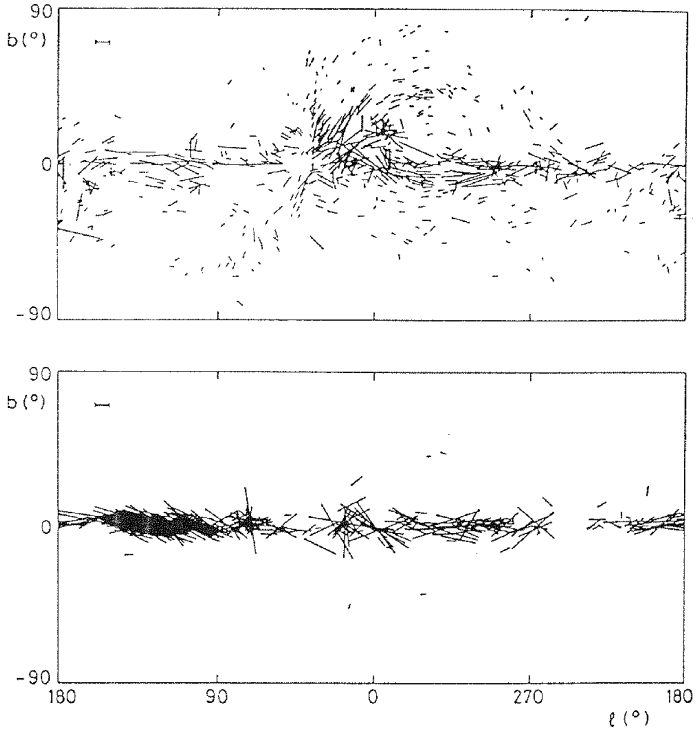

Figure 1.10 The direction of the magnetic field of the Galaxy as measured through optical polarization of starlight. Upper panel: stars within 400 pc, emphasizing the magnetic field associated with local clouds. Lower panel: stars between 2 and 4 kpc, showing some regions with magnetic field parallel to the galactic plane while others are more random. Figure reproduced with permission from D. S. Mathewson and V. L. Ford, 1970, *Mem. R. A. S.*, **74**, p. 139.

of about 1.5 μG in the solar neighborhood and has two field reversals within the solar circle and one outside. The field may show a spiral structure where the reversals occur in the interarm regions. There is also a considerable non-uniform magnetic field, partly associated with expanding interstellar shells (superbubbles) and their shocks. The strength of the magnetic field increases inside dense clouds, $B \sim n^{\alpha}$ with $\alpha \simeq 0.5$ and typically $B \simeq 30\,\mu\text{G}$ at $n \simeq 10^4\,\text{cm}^{-3}$. The direction of the field is correlated over the entire extent of the cloud from the diffuser outer parts to the denser cores.

1.3.3 Cosmic rays

High energy ($\gtrsim 100\,\text{MeV nucleon}^{-1}$) particles contribute considerably to the energy density of the ISM ($\simeq 2\,\text{eV cm}^{-3}$; Table 1.2). Cosmic rays consist mainly of relativistic protons with energies between 1 and 10 GeV, 10% helium, and

heavier elements and electrons at about the 1% level. The relative abundance of the elements in the cosmic rays is non-solar, attesting to the importance of spallation–production of light elements and an origin either in material of stellar (perhaps SN) composition or in sputtered interstellar grains. The interaction of energetic (1–10 GeV) cosmic-ray protons with interstellar gas gives rise to gamma rays with $E_\gamma \gtrsim 50$ MeV through π^0 meson decay emission. Likewise, the interaction of energetic (<1 GeV) electrons with interstellar gas gives rise to gamma rays through bremsstrahlung and inverse Compton scattering. Gamma ray observations, in combination with interstellar gas surveys, can therefore be used to measure the distribution of cosmic rays in the Galaxy. Cosmic rays are tied to the galactic magnetic field and confined to a disk of radius 12 kpc with a thickness of ~2 kpc. Cosmic rays seem to draw their energy from supernovae with an efficiency of about 10% of the kinetic energy of the ejecta. The pressure due to these cosmic rays provides support against gravity for the gas in the ISM.

Low-energy ($\simeq$100 MeV) cosmic rays are important for the heating and ionization of interstellar gas. Unfortunately, their flux is difficult to measure within the heliosphere because of strong modulation by the solar wind. The measured cosmic-ray flux near the Earth is shown in Fig. 1.11 together with a fit based upon a model for the cosmic-ray injection spectrum and energy-dependence of the residence time in the interstellar medium. It is obvious that the correction is substantial at low energies. While the interstellar cosmic-ray flux is difficult to measure directly, the resulting ionization drives the build-up of simple molecules (e.g., OH), which can be studied (Section 8.7). These indirect measurements imply a primary cosmic-ray ionization rate in the ISM of $\zeta_{\rm CR} \simeq 2 \times 10^{-16}$ (H atom)$^{-1}$ s^{-1}. Localized regions of much higher ionization rate may occur near associations of massive stars.

1.3.4 Kinetic energy of the ISM

Winds from early-type stars and supernovae explosions supply bulk kinetic energy to the ISM. Compared to the stellar radiative budget, the total mechanical energy output is only small, ~0.5 % (Table 1.2). However, the turbulent energy of the HI is about 6×10^{51} erg kpc^{-2} in the solar neighborhood and provides support for the HI gas against gravity. The HI also shows ordered vertical flow, at some 5 km s^{-1} in the Milky Way, as well as the infall of large gas complexes at higher latitudes.

The expanding shells blown by individual stars and the superbubbles blown by the concerted action of OB associations have an important influence on the morphology of the ISM. They sweep up and compress the surrounding ISM

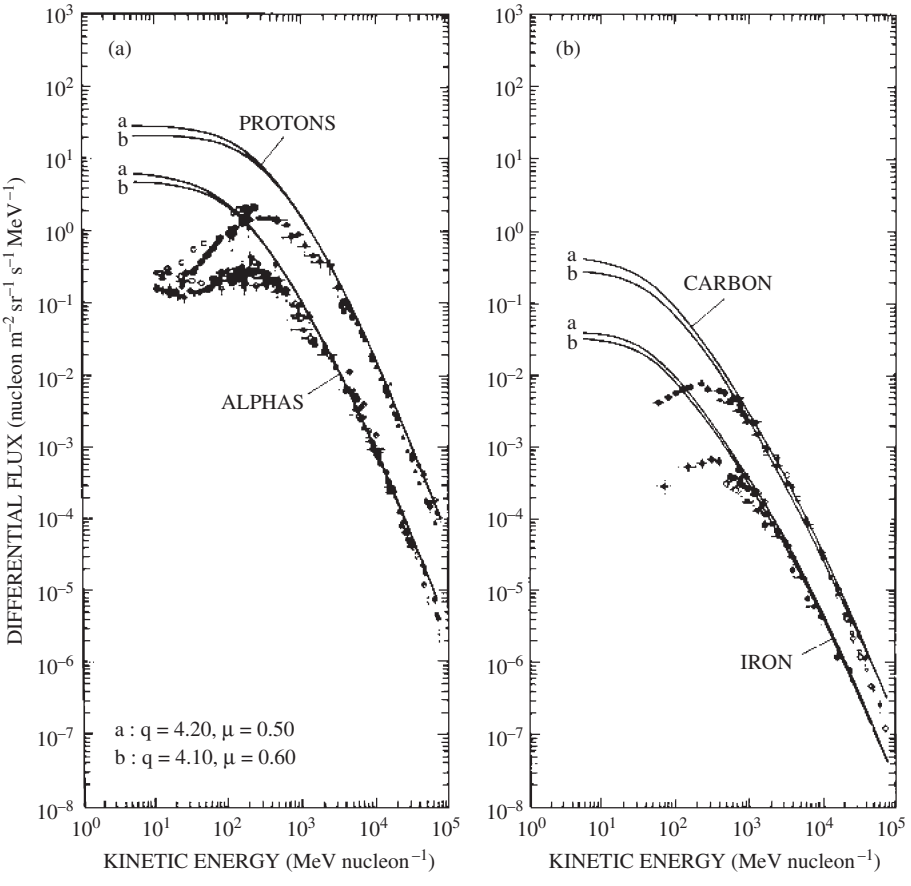

Figure 1.11 The cosmic-ray proton flux as a function of energy measured near the Earth and the inferred interstellar cosmic-ray flux after the effects of modulation by the solar wind have been taken into account. Figure reproduced with permission from W.-H. Ip and W. I. Axford, 1985, *A. & A.*, **149**, p. 71.

and set it into motion. These motions are often unstable to Rayleigh–Taylor and Kelvin–Helmholtz instabilities and, in general, turbulence is expected to take over. This kinetic energy decays through shock waves when clouds collide, emerging as line radiation, or through the excitation of plasma waves, which, eventually, also heat the gas. The average heating due to turbulence is, however, small (Table 1.2).

On a smaller scale, individual molecular clouds show linewidths in excess of the thermal width because of the presence of turbulent motions. This turbulence, which is probably of a magneto-hydrodynamic nature, supports these clouds against self-gravity. This turbulent energy is supplied by powerful outflows driven by newly formed stars into their surroundings – and hence derives from the

gravitational energy of the collapsing cloud core – or by direct tapping of the magnetic or rotational energy supporting the cloud.

1.3.5 Summary

While these energy sources are very similar in magnitude (cf. Table 1.2), how much each of them contributes to the heating of the gas (and dust) depends on the coupling processes. Understanding these processes will thus be of prime importance for understanding the physical state of the ISM.

1.4 The Milky Way

Table 1.3 summarizes several characteristics of the Milky Way as a galaxy. Comparing these with those of other galaxies, the Hubble type of the Milky Way seems to be somewhere between an Sb and an Sc. In many ways, the Milky Way seems to be an average spiral galaxy.

1.4.1 Galactic distribution

The molecular gas shows an exponential distribution, peaking at the molecular ring ($\simeq$4.5 kpc) with a scale length of about 3 kpc. In contrast, the atomic gas has a rather flat distribution out to about 18 kpc (cf. Fig. 1.12). So, within the solar circle, the surface density of the molecular gas is somewhat larger than that of the atomic gas. In contrast, the atomic gas dominates the molecular gas by far in the outer Galaxy. Within 4 kpc, there is a hole in both the atomic and molecular gas distribution except for the nuclear ring in the inner Galaxy. The total HI mass is about 5 times that of H_2.

The most striking aspect of the gas and dust distribution of any galaxy is the thinness of the disk. The molecular gas has a thickness of $\simeq$75 pc compared with a radial scale length of 4 kpc. In the inner Milky Way, the HI scale height is two to three times larger, depending on which neutral gas component is considered. In the outer Galaxy, the neutral gas disk flares to a thickness of about 1 kpc. Nevertheless, this is still small compared to the radial scale length. The gas disk also shows a warp in the outer Galaxy.

1.4.2 Spiral structure

It is difficult to discern the spiral structure of our Galaxy from the atomic gas distribution because of the presence of non-circular velocity components. Molecular clouds are better tracers; not least because molecular clouds are more

Table 1.3 *The Milky Way*

Object	Mass ($M_\odot$)
Stars	1.8 (11)
Gas	4.5 (9)

Source	Luminosity ($L_\odot$)
Stellar luminosities	
All stars	4.0 (10)
OBA	8.0 (9)
Gas and dust	
[CII] 158 μm	5.0 (7)
FIR	1.7 (10)
Radio	1.5 (8)
γ-rays	3.0 (5)
Mechanical luminosities	
SN	2.0 (8)
WR	2.0 (7)
OBA	1.0 (7)
AGB	1.0 (4)

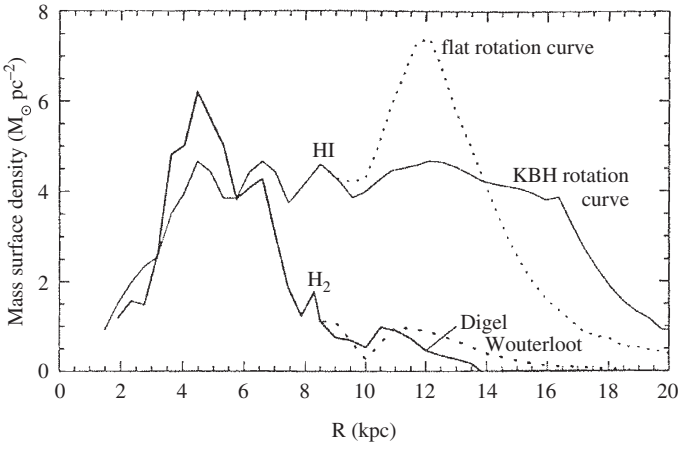

Figure 1.12 The mass surface density of HI and H_2 as a function of galactocentric radius. The distribution of HI in the outer Galaxy is quite sensitive to the adopted galactic rotation curve. Note that the nuclear ring is not shown. Figure reproduced with permission from T. M. Dame, 1993, in *Back to the Galaxy*, ed. S. S. Holt and F. Verter (New York: AIP), p. 267.

limited to the arms. Long structures are present in either tracer and, for example, the Sagittarius–Carina arm is readily recognized. Nevertheless, whether the Milky Way is a two-arm or four-arm spiral has not been settled.

1.4.3 Spiral galaxies

The overall distribution of the ISM can be particularly well studied in other nearby galaxies such as M31. This shows that the bright HII regions, the atomic and molecular gas, and the dust are concentrated in spiral arms. In contrast the interarm regions are much less obscured, although diffuse HI is present throughout the disk as well. Edge-on galaxies such as NGC 891 – an Sb galaxy very similar to our own – show most clearly the narrow disk component; for example, in the dust absorbing background stellar light. The HI distribution of this galaxy shows a component that is somewhat more extended than that of the Milky Way.

1.5 The mass budget of the ISM

Stars of all masses in various stages of their lives indiscriminately pollute their environment with gas, dust, and metals. Except for a few elements produced in the Big Bang, the abundance of all heavy elements reflects this enrichment with stellar nucleosynthetic products. Table 1.4 summarizes gas and dust mass injection rates into the ISM for a variety of stellar objects. The dust budget has been split out into two separate columns according to whether the stellar source contains carbon-rich zones (C/O > 1), which lead to carbonaceous dust formation, or oxygen-rich zones, which lead to the formation of oxides (silicates) or metals. The quoted values are uncertain – some more than others – and are often based upon various assumptions. Even estimates of the relative importance of high-mass stars versus low-mass stars evolve over time because of new developments in, for example, the determination of mass loss rates (e.g., IR studies) or nucleosynthetic reaction rates (e.g., the $^{12}C(\alpha, \gamma)^{16}O$ rate). Thus, while 20 years ago high-mass stars ($M > 8\,M_{\odot}$) were thought to be mainly responsible for the carbon in the interstellar medium, in more recent studies carbon-rich red giants dominate. These injection rates also vary across the Galaxy; i.e., because of the general increase in metallicity towards the inner Galaxy, the ratio of the O-rich to C-rich giants increases towards the galactic center, as does the Wolf–Rayet star population.

The gas mass return rate is dominated by low-mass red giants, as expected, since low-mass stars dominate the stellar mass of the Galaxy. However, massive stars are more efficient in producing and injecting heavy elements, such as O and Si, in the ISM (a typical type-II supernova has an enrichment factor of $\sim$10 for such elements). However, on the AGB, low-mass stars inject much C formed

Table 1.4 *Interstellar gas and dust budgets*

Source	$\dot{M}_H^a$ ($M_\odot$ kpc^{-2} Myear^{-1})	$\dot{M}_c^b$ ($M_\odot$ kpc^{-2} Myear^{-1})	$\dot{M}_{sil}^c$ ($M_\odot$ kpc^{-2} Myear^{-1})
C-rich giants	750	3.0	—
O-rich giants	750	—	5.0
Novae	6	0.3	0.03
SN type Ia	—	0.3[d]	2[d]
OB stars	30	—	—
Red supergiants	20	—	0.2
Wolf–Rayet	100[e]	0.06[f]	—
SN type II	100	2[d]	10[d]
Star formation	−3000	—	—
Halo circulation[f]	7000		
Infall[g]	150		

[a] Total gas mass injection rate.
[b] Carbon dust injection rate.
[c] Silicate and metal dust injection rate.
[d] Fraction and composition of dust formed in SN is presently unknown. These values correspond to upper limits.
[e] Dust injection only by carbon-rich WC 8–10 stars.
[f] Mass exchange between the disk and the halo estimated from HI in non-circular orbits and CIV studies.
[g] Estimated infall of material from the intergalactic medium and satellite galaxies.

by the triple-α process. Asymptotic giant branch stars are also the site of the production of the s process (formed through slow neutron capture) elements. Type-Ia supernovae, which also have low mass progenitors, inject a considerable amount of Fe into the ISM.

The time scale for stars to inject or replenish the local interstellar gas mass (8×10^6 $M_\odot$ kpc^{-2}) is $\simeq 5 \times 10^9$ years. The total dust injection rate corresponds to a dust-to-gas ratio in the ejecta of ∼1.5%. This is somewhat larger than the average dust-to-gas ratio in the ISM, reflecting the synthesis of heavy elements in type-II supernova. Locally, star formation will convert all molecular gas into stars in only 2×10^8 years; the average star formation rate is heavily weighted towards the inner molecular ring. The different phases of the ISM exchange material at a rapid rate (3×10^7 years) and, considering all the available gas, this time scale to convert gas into stars increases to $\simeq 3 \times 10^9$ years and is more comparable to the stellar injection time scale. Both rates are very short compared with the lifetime of the Galaxy ($\simeq 1.2 \times 10^{10}$ years). The disk of the Galaxy also exchanges material with the lower halo. In particular, the concerted action of supernovae set up a galactic fountain and some 5 $M_\odot$ is exchanged per year. In terms of the mass flux, this circulation pattern dominates the mass budget. Finally, the Galaxy is still accreting primordial material from its environment. The amount

of this accretion is controversial. There is a contribution from satellite galaxies such as the Magellanic Clouds, and the Magellanic Stream represents an accretion of some $150\,M_\odot$ kpc^{-2} Myear^{-1}. There are also some indirect arguments that suggest that the Galaxy may have been accreting about 1 $M_\odot$ year^{-1} of metal-poor primordial gas over much of its lifetime or about an order of magnitude more than the Magellanic Stream accretion.

1.6 The lifecycle of the Galaxy

The origin and evolution of galaxies are closely tied to the cyclic processes in which stars eject gas and dust into the ISM, while at the same time gas and dust clouds in the ISM collapse gravitationally to form stars. The ISM is the birthplace of stars, but stars regulate the structure of the gas, and therefore influence the star formation rate. Winds from low-mass stars – and hence, the past star formation rate – control the total mass balance of interstellar gas and contribute substantially to the injection of dust, an important opacity source, and polycyclic aromatic hydrocarbon molecules (PAHs), an important heating agent of interstellar gas. High-mass stars (i.e., the present star formation rate) dominate the mechanical energy injection into the ISM, through stellar winds and supernova explosions, and thus the turbulent pressure that helps support clouds against galactic- and self-gravity. Through the formation of the hot coronal phase, massive stars regulate the thermal pressure as well. Massive stars also control the FUV photon energy budget and the cosmic-ray flux, which are important heating, ionization, and dissociation sources of the interstellar gas, and they are also the source of intermediate-mass elements that play an important role in interstellar dust. Eventually, it is the dust opacity that allows molecule formation and survival. The enhanced cooling by molecules is crucial in the onset of gravitational instability of molecular clouds.

Clearly, therefore, there is a complex feedback between star formation and the ISM. And it is this feedback that determines the structure, composition, chemical evolution, and observational characteristics of the interstellar medium in the Milky Way and in other galaxies all the way back to the first stars and galaxies that formed at redshifts, $z, > 5$. If we want to understand this interaction, we have to understand the fundamental physical processes that link interstellar gas to the mechanical and FUV photon energy inputs from stars.

1.7 Physics and chemistry of the ISM

The key point always to keep in mind when studying the interstellar medium is that the ISM is far from being in thermodynamic equilibrium. In thermodynamic equilibrium, a medium is characterized by a single temperature, which describes

the velocity distribution, excitation, ionization, and molecular composition of the gas. While the velocity distribution of the gas can generally be well described by a single temperature, the excitation, ionization, and molecular composition are often very different from thermodynamic equilibrium values at this temperature. This reflects the low pressure of the ISM, so that, for example, collisions cannot keep up with the fast radiative decay rates of atomic and molecular levels. Ionization and chemical composition are also kept from their equilibrium values by the presence of ∼100 MeV cosmic-ray particles – clearly a non-Maxwellian component – and a diluted, stellar, EUV-FUV photon field, which is much stronger than a 100 K medium would normally have. Finally, the large-scale velocity field is much influenced by the input of mechanical energy.

Whenever a gas is not in local thermodynamic equilibrium, the level populations, degree of ionization, chemical composition, and of course the temperature are set by balancing the rates of the processes involved. Much of the study of the ISM is thus concerned with identifying the various processes that control the ionization and energy balance, setting up the detailed statistical equilibrium equations and solving them for the conditions appropriate for the medium.

In the remainder of this book, we will thus first study the physical and chemical processes that are of astrophysical relevance (Chapters 2–4). This is followed by a discussion of the physics and chemistry of two important components of the ISM: dust grains (Chapter 5) and large molecules (Chapter 6). With this in hand, we can examine in-depth HII regions, the phases of the ISM, photodissociation regions, and molecular clouds (Chapters 7–10). In each chapter, the ionization and thermal balance are investigated first, setting up the statistical equilibrium equations and deriving the relevant parameters of the medium. This is then followed by a discussion of the observations of these objects and their analysis. In Chapters 11–12, non-equilibrium effects of a different nature are studied. Specifically, the time-dependent effects of strong shock waves on the temperature and chemical composition of clouds are discussed in Chapter 11. Chapter 12 examines then the dynamical effects of expanding HII regions, supernova explosions and stellar winds. Finally, in Chapter 13, some aspects of the lifecycle of interstellar dust – which is a prime example of these types of non-equilibrium effects – are explored.

1.8 Further reading

A general, technical yet accessible, introduction to the interstellar medium is provided by [1].

An introductory-level discussion of the interstellar medium can be found in [2]. A thorough but now dated monograph on physical processes in the interstellar medium is [3], which is an updated version of [4]. These two textbooks are

no easy reading matter and the reader should beware that many a promising young scientist was last observed buying these books. A recent monograph on the interstellar medium is [5], which is intended for postgraduate courses. An unsurpassed textbook treating the physics of ionized gas is [6].

A recent overview of the properties of our Galaxy as compared to other galaxies is given by [7].

Panoramic images of the Milky Way at different wavelengths can be found on the web, http://adc.gsfc.nasa.gov/mw/milkyway.html.

Each of these wavelengths traces a different component of the Galaxy. It is instructive to compare these different images.

References

[1] J. B. Kaler, 1997, *Cosmic Clouds: Birth, Death, and Recycling in the Galaxy*, (New York: Freeman Co.)
[2] J. E. Dyson and D. A. Williams, 1980, *Physics of the Interstellar Medium* (Manchester: Manchester University Press)
[3] L. Spitzer, Jr., 1978, *Physical Processes in the Interstellar Medium* (New York: Wiley)
[4] L. Spitzer, Jr., 1968, *Diffuse Matter in Space*, (New York: Interscience)
[5] M. A. Dopita and R. S. Sutherland, 2003, *Astrophysics of the Diffuse Universe*, (Berlin: Springer Verlag)
[6] D. Osterbrock, 1989, *Astrophysics of Gaseous Nebulae and Active Galactic Nuclei* (Mill Valley: University Science Books)
[7] R. C. Kennicutt, 2001, in *Tetons 4: Galactic Structure, Stars and the Interstellar Medium*, ed. C. E. Woodward, M. D. Bicay, and J. M. Shull (San Francisco: ASP), p. 2